Egyptian Journal of Soil Science

http://ejss.journals.ekb.eg/

A Modified Equation for Fitting the Shape Feature of the Entire Soil Water Characteristic Curves

Wail M. Omran[a*], Ahmed A. M. Awad[b], Atef A. A. Sweed[b] and Taia A. Abd El –Mageed[c]

[a]*Department of Soil Science, Faculty of Agriculture, Menoufia University, Menoufia, Egypt*

[b]*Soil and Natural Resources Department, Faculty of Agriculture and Natural Resources, Aswan University, Aswan 81528, Egypt*

[c]*Soil and Water Department, Faculty of Agriculture, Fayoum University, Fayoum 63514, Egypt*

THE PRESENT WORK aims to modify Fredlund and Xeng (FX) model to simulate the soil water characteristic curve (SWCC) to be applicable in soil physics and agriculture. Laboratory measurements of the SWCC of clay soil, representing the soil type close to river Nile in Egypt, were carried out using a pressure plate extractor. The measured points of the curve include saturation, field capacity (FC), and permanent wilting point (PWP). The estimation of the regression equations and unknown parameters was performed using non-linear estimation in the STATISTICA program through user-specified regression. The flexibility and capability of the proposed equation (PE) for a wide range of soil suction (ψ) values and soil types were also determined. The SWCC of the experimental soil and statistical tools indicated that PE showed a very good fit to the measured data. The three compared models accurately simulated the entire range of SWCCs for different soil textures. The statistical analysis and fitting curves revealed that the PE precisely simulated the SWCCs for the entire range of ψ values for different soil types and performed better than MVG and FX. Furthermore, only PE was able to simulate SWCCs using different forms of soil moisture, distinct from MVG and FX. The study hence recommends the use of the PE in simulating SWCCs.

Keywords: Empirical models, Soil water characteristic curve, Fredlund and Xing model.

1. Introduction

For decades, one of the most popular subjects has been water saving; however, in agriculture scientific irrigation scheduling and management is the only approach for that purpose. Therefore, understanding and evaluating water status under an unsaturated condition is of utmost importance. Soil water characteristic curves (SWCCs) can be used to describe unsaturated soil behavior. In this respect, (Rousseva et al., 2017; Bassouny and Abbas, 2019; Elhusieny et al., 2020; Sheta and Fayed, 2021) reported that an SWCC is related to almost all soil properties and can be used for accurately assessing the water storage capacity, pore size distribution, and hydraulic conductivity of unsaturated soil. The curve is therefore involved, directly and indirectly, in calculating the irrigation requirement, soil water balance, and irrigation intervals based on knowledge of the field capacity (FC), the permanent wilting point (PWP), the actual soil water content, the amount of water input and output, and acceptable water depletion in the root zone depending on the critical crop yield. The vadose zone, particularly the root zone, represents unsaturated, near-saturated, and saturated soil; however, unsaturated soil is the common condition. Under such a condition, the soil water content (WC) is retained by a negative pressure known as matric potential or soil suction (ψ). The relationship between WC and ψ is the SWCC. The curve determination requires direct and continuous

*Correspondence: wael.omran@agr.menofia.edu.eg or womran@yahoo.com; Tel.: (00201068228994).
Received: 23/09/2022; Accepted: 30/11/2022
DOI: 10.21608/EJSS.2022.164765.1541

measurements of both WC and ψ, which are costly and time-consuming (Achieng, 2019). In addition, the water status of unsaturated soil is difficult to monitor because it undergoes irregular dynamic changes since it is governed by the hydraulic gradient, a function of both WC and ψ. Moreover, pore size, geometry distribution and the type of clay are influential factors. To practically model, an SWCC, initial and boundary conditions that need to be simulated should be defined, and multicomponent mathematical processes need to be resolved. Empirical models should be more effective and reliable for this purpose than theoretically based ones. Additionally, there is currently no generally acceptable, applicable, and precise hypothetically based model describing SWCCs. Although Smith and Mullins (2001) and Eyo et al. (2020) included all common laboratory methods in determining SWCCs and the associated ψ range, there is no method that can be used to determine the full range of SWCCs; i.e., from 0 to 106 kPa. Therefore, two or more methods should be used, and the two measured components should be combined to develop the full-range curve, which makes the situation more difficult.

The general features of SWCCs show, at saturation and near saturation, that WC does not change with increasing ψ, which is followed by a very rapid decrease in WC with any small increase in ψ, and the change in WC gradually slows and then stops. The common SWCC therefore usually has two bending or inflection points. Some curves, however, have one point or more than two points depending on the soil texture. The relationship is thus extremely nonlinear. The first inflection point is associated with the soil water potential at bubbling pressure or the air entry value, which refers to ψ where the air starts to enter the largest soil pores. The second inflection point is at the ψ value associated with the residual water content (RWC), which is defined as the WC when soil hydraulic conductivity is zero. Another specific definition of RWC is the WC corresponding to the asymptote of the SWCC of hygroscopic water or air-dried soil. At this point, a large change in ψ is required to remove additional water from the soil. The total ψ corresponding to RWC appears to be essentially the same for all types of soils, i.e., 106 kPa (Fredlund and Xing, 1994; Tinjum et al., 1997; Leong and Rahardjo, 1997; Sillers and Fredlund, 2001). Fredlund et al. (2011) presented the general shape features of the entire SWCC, with WC expressed on a mass basis and ψ in kPa units. The relationship is usually expressed on a semi-logarithmic (log ψ) versus a normal scale of WC to show the curve details because of the large range of ψ values. This relationship is typically determined experimentally and is represented graphically by the SWCC. However, a successful model is difficult to establish because of the physical meanings of the parameters required to simulate the inflection points. In addition, other problems affect the capability and suitability of models, including the following: models may not be sufficiently rigorous, input soil properties may not necessarily be known, altered initial and boundary conditions may not be sufficiently defined, and the computed results might not be properly interpreted (Fredlund and Xing, 1994; Leong and Rahardjo, 1997; Gitirana and Fredlund, 2004).

Many different equations have been developed to predict SWCCs (e.g., Burdine, 1953; Gardner, 1958; Brooks and Corey 1964; Brutsaert, 1966; Visser, 1968; Farrel and Larson, 1972; Campbell, 1974; Maulem, 1976; van Genuchten, 1980; William et al., 1983; Saxton et al., 1986; Fredlund and Xing, 1994; Kosugi, 1994; Assouline et al., 1998). Each equation has its own limitation. A discussion of the most common SWCCs is required for a reasonable comparison.

The Gardner (1958) model was originally proposed for defining unsaturated hydraulic conductivity, and its application to the SWCC is inferred. Campbell (1974) attempted to reduce the number of fitting parameters in the Gardner model by setting a specific parameter equal to ψ at air entry. Such an approximation reduces the capability of the model in fitting the data. The models of Burdine (1953), Brutsaert (1966), and Maulem (1976) could be considered special cases of the more general form of the model presented by Van Genuchten, 1980 (VG). Fredlund and Xing, 1994 (FX) suggested leaving m and n in VG with no fixed relationship in order to obtain more flexibility. The three-parameter VG (without the condition of m=1-1/n) is the considered form and is named the modified VG (MVG).

This study does not include the equations associated with the specified range of matric potential (up to PWP), such as Assouline et al. (1998), and the equations depending on particle size distribution, such as Saxton e t al. (1986) and Kosugi (1994), or equations that require measurements of specific soil properties (e.g., soil porosity), such as Visser (1968). Moreover, the equations, which have two forms depending on the air-entry value, such as Brooks and Corey (1964), and the equations that essentially require the determination of RWC, where the changes may affect the originality of the model, such as Gardner (1958), are not included. In this respect, Leong and Rahardjo (1997) performed a comparative study of

SWCC equations and reported that the models of Farrel and Larson (1972) and William et al. (1983) did not present a sigmoidal curve. In addition, it is important to mention that the curve-fitting equation could be improved if values of ψ, which is less than the air-entry value, are omitted. Such task was not adopted because our objectives were the full curve determination and a comparison of the equations based on similar conditions. Therefore, the models required special measurements of soil properties, and the models with technical disadvantages were considered out of the comparison (El-Nady, 2015 and Elbana et al., 2019).

It is worth emphasizing that fewer the equation fitting parameters, the lower the accuracy and flexibility of the equation form and vice versa. Therefore, complex equations are appropriate if required and if they are able to be calculated. In this respect, Fredlund et al. (1994) mentioned that when the number of measurements exceeds the number of fitting parameters, a curve-fitting procedure can be applied to determine the fitting parameters. The FX model has three parameters: α, n, and m; where α is related to the ψ at air-entry, n mainly influences the desaturation rate in the transition zone of an SWCC or the slope of the curve, and m controls the RWC (Rahimi et al., 2015 and Chai and Khaimook, 2020). Fredlund and Xing (1994) introduced correction function for the FX model to calculate the RWC. The physical meaning of soil parameters should be different alternative after establishing the empirical equation and obtaining a good fit with measured data. Therefore, the challenge of the desired model is its capability in simulating the entire SWCC over a wide range of soil textures.

Among the above-reviewed SWCC models, only MVG and FX were suitable for inclusion in the study since they are general forms, do not require the determination of special soil properties, and can be used to simulate the curve for the full ψ range for various soil types.

Our goals were to simulate SWCC without the inclusion of difficult mathematical processes and problematic simulations of complex soil matrices and also to avoid the measurement of numerous soil properties; however, detailed measured data and mathematical equations appropriate for Egyptian soils are still not available.

The objectives of the study were to introduce a new equation with parameters related to the shape features of the SWCC in order to achieve the best possible fit for Egyptian clay soil, to test the applicability and flexibility of the proposed equation (PE) over a wide range of ψ values and soil textures compared with MVG and FX models, and to overcome the difficulties in deriving and solving mathematical equations by presenting a simple calculation procedure.

2. Materials and methods

Soil analysis and SWCC measurements

Surface soil samples were collected from the experimental farm of the Faculty of Agriculture, Menoufia University, Menoufia, Egypt. The samples were air-dried and sieved using a 2 mm sieve. The RWC was calculated. The soil particle size distribution was determined using the pipette method. Also, three replicates of undisturbed soil samples, one for each measured point, were used to determine the drying curve of the SWCC in the laboratory using a pressure plate extractor (PPE). In the PPE method, air pressure is applied above the soil samples (cores containing soil) to remove water from the soil samples (the ceramic plate allows only water to move through and does not allow air to pass). The undisturbed samples, collected using soil cores (26 mm diameter and 10 mm height), were completely saturated and placed on the ceramic plate extractor Dane (2002).

After equilibrium with the applied pressure, the samples were removed and their volumetric WC (θ) was determined via multiplying WC in mass bases by soil bulk density. The FC and PWP were determined at ψ values of 33 and 1500 kPa, respectively. Table 1 shows the calculated particle size distribution, bulk density, and total porosity. The measurements described above were performed according to Black et al. (1965) and Pansu and Gautheyrou (2006).

Table 1. Physical analysis of the studied soil.

Coarse sand	Fine sand	Silt	Clay	Texture	Bulk Density ($g.cm^{-3}$)	Total Porosity
1.50	27.23	29.05	42.22	Clay	1.24	0.54

Statistical and mathematical calculation procedures

To avoid complicated deferential and integral procedures and to prevent graphical errors, the unknown parameters for all studied equations were solved by suitable computer program. The calculation was performed using the advanced nonlinear estimation solver in STATISTICA software Ver. 12.5 (The original author is Stat-Soft and the developer is TIBCO; http://www.tibco.com/data-science-and-streaming).

The unknown parameters for all studied equations were calculated through user-specified regression. The program calculates the standard errors of the estimated unknown parameters. These standard errors were based on the second-order partial derivatives for the parameters, which were computed via finite difference approximation. In some circumstances, the estimation could not proceed as a result of the logarithm of an independent variable that returned a value of zero (as the case of both MVG and FX models), and the data could not be calculated. If the data could not be fit to the regression model, the iterative estimation procedure failed to converge, producing very large or very small parameter estimates (Lourakis, 2005 and Gavin, 2019). In order to solve such problem, user-specified regression was performed, and loss function (LF) included a penalty assessment designed to penalize the unknown parameters if either one was equal to zero as follows:

$$LF = (observed\text{-}\ predicted)^2 + (a<0) \times 100000 + (b<0) \times 100000$$

Quasi-Newton, simplex, Hooke–Jeeves pattern moves, and Rosenbrock's pattern search were the available methods for the nonlinear estimation of the user-specified regression model. Among the methods available for calculation, there was one method that was able to calculate all the equations for all the data, which is the simplex method. Therefore, the simplex method was used to calculate the unknown model parameters.

Such an estimation procedure is effective in minimizing the LF and calculating the best set of parameters to obtain the best possible fit of the desired model. The method begins with a particular set of initial estimates (start values); in the first iteration, the step size determines the amount by which the parameters will be changed. Additionally, the simplex method was adopted to compute the slope of a function at a particular point as the first-order derivative of the function. The slope of the slope is the second-order derivative, which indicates how fast the slope changes at the respective point and in which direction. A very useful and detailed discussion on nonlinear estimation methods can be found in the STATISTICA Electronic Manual (program help panel).

Model evaluation and validation

Most SWCC models include dimensionless WC or the normalized water content (NWC), i.e.,

$$NWC = \frac{Actual\ WC\ -\ RWC}{Saturated\ WC\ -\ RWC}$$

Alternatively, values relative to WC at saturation or effective saturation (ES), i.e.,

$$(ES = \frac{Actual\ WC}{Saturated\ WC}) \approx \frac{Actual\ WC}{maximum\ value\ of\ WC},$$

can be used rather than NWC according to the simplification suggested by van Genuchten et al. (1991) and Tinjum et al. (1997). However, setting NWC equal to ES assumes that RWC is equal to zero when the full curve data are not available; this is also done to ensure accuracy in the graphical determination. This assumption is in agreement with that proposed by van Genuchten et al. (1991) and Tinjum et al. (1997).

Therefore, for generalization purposes and to eliminate the need to include the saturation and RWC values, if not exist, the WC of all studied equations was converted to relative WC and considered equal to ES. ES was taken as the dependent variable since the WC changes in response to the applied ψ in the desorption SWCC were obtained in the study. All the necessary mathematical calculations were performed.

The most common algorithm (i.e., Quasi-Newton procedure) was employed in developing the PE, through rearranging FX model and adding one more constant. The calculation was done by testing different mathematical forms and doing several iterations until reach the most accurate form in simulating the measured SWCC data.

Three statistical tools, i.e., LF, the correlation coefficient (r), and coefficient of determination (R^2), were used to evaluate and validate the studied models. The following explanations were used to determine the importance of each studied statistical tool.

Measured values = fitted values ± residual

Residual = LF = squared difference between measured and calculated values = (observed – predicted)^2

LF was helpful in evaluating how well the model fit the data set. The calculation was done using STATISTICA program.

r is the correlation between two variables (X and Y); So, r always takes values between -1 and 1 and is intended to quantify how strongly a pair of variables are related. The calculation, of r, was done using CORREL function in Excel program of measured and predicted ES or θ values.

The coefficient of determination, R^2, measures how the variance of y is explained graphically by the regression model and if the model simulates values close to the actual values. The calculation was done using STATISTICA program.

3. Results and discussion

Measured data of SWCCs and PE

The following expression (PE) was developed through adapting the FX model and introducing another constant, in order to obtain the best fit to measured SWCC of clay soil, collected from the delta of River Nile of Egypt (Fig. 1).

The PE is also validated through a wide range of both soil textures and suction (Fig. 2-6 and appendix A). In this respect, Elbana et al. (2019) suggested conducting further studies in different agro-ecological areas in Egypt to optain more precise model calibration and validation. The PE was tested based on actual measurements of the SWCC between 0 and 1500 kPa suction for a clay soil (Fig. 1) as described in the materials and methods:

$$ES = \frac{1 - b}{\left\{1 + [\frac{ln\,(\psi+1)}{\alpha_1}]^{n_1}\right\}^{m_1}} \approx \theta$$

where b, α_1, n_1, and m_1 are free unknown parameters. The measured data and simulated curves (i.e., ES in the main axis and θ in the secondary axis) are presented in Fig. 1 (A and B). Resulted equations and obtained r, R^2, and LF values are presented in Fig. 1 A. High values of r and R^2 and low values of LF (Fig. 1 A) were indicated, which ensure the applicability of PE in simulating SWCC using both ES and θ. Fig. 1 B shows the same curves with x axis in log scale, rather than normal scale (as in Fig. 1 A), to show the curve changes in detail and to display the inflection points if exist. The zero value of suction was changed to 0.01 in fig. 1 B to calculate logarithm, such approximation not affect the shape of the curve. The first inflection point (air entry value, which is close to FC) occurred between 20 and 300 kPa (Fig. 1).

The result agrees with Jiang et al. (2020), who reported that when the matrix ψ increased to 200 kPa, the curve tended to be steady and the drying rate decreased. From Fig. 1 FC and PWP were at volumetric WC about 42% and 0. 23 %, respectively. The PE was presented due to the absence of SWCC-based models of soils of Egypt; Therefore, PE was developed using clay soil to represent the types of soil of the Wadi and the Delta of the Nile River in Egypt. The calculation requires only ψ and WC data.

As the SWCC is a complex nonlinear relationship, the key of nonlinear curve fitting estimation is to calculate the coefficients that minimize the residual variance or LF around the regression line. It is therefore imperative to develop a special mathematical relationship. However, no known mathematical function that is a built-in function of the commercial computer program can successfully describe such a relationship, especially across the full range of the curve.

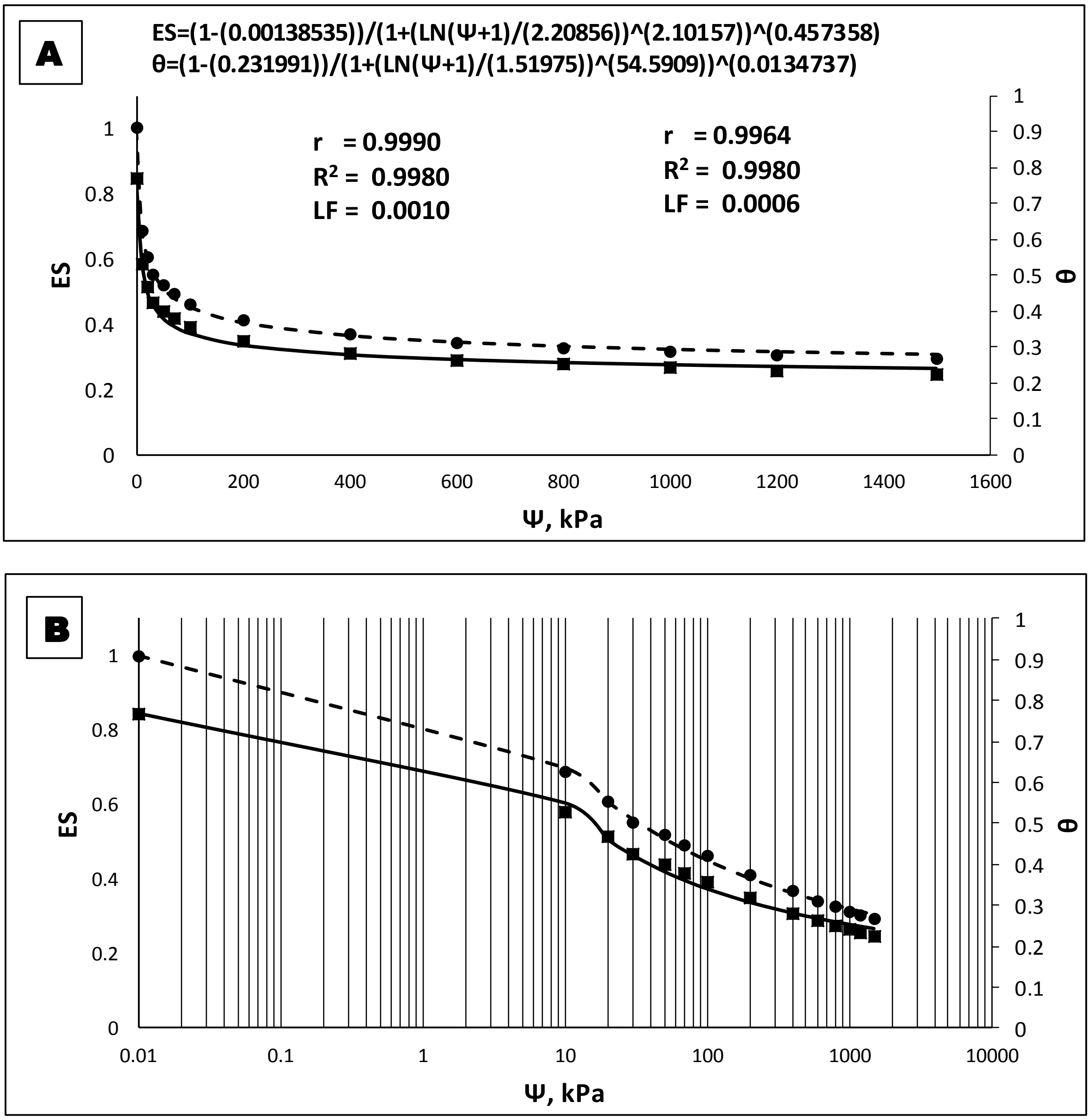

Fig. 1. Measured and calculated SWCC of the studied Egyptian clay soil (normal and log scales) using PE.

The PE was developed to simulate two inflection points and three lines; two of them were horizontal lines that described the saturation or WC at a ψ value lower than the air-entry, while the other line described the RWC, and the third line described the slope of the main curve between air entry and RWC. In order to achieve such three regression lines, the first attempt used a logistic function or pearl curve function because this function is already built into the commercial computer programs and represents a shape similar to the SWCC. Unfortunately, the function did not fit the data at all. The other option was a user-specified equation representing an S-curve that fit the data across the entire range of ψ values that did not require special measurements of soil properties (i.e., only ψ and WC). For that reason, the PE was formed.

The PE is essentially empirical, similar to many earlier models. The PE could be considered another form of the FX model. The FX was developed using WC on a mass basis, which is suitable for geotechnical and civil engineering applications. The PE is adopted to use WC on a volume basis, which is the term used in soil physics, agriculture and irrigation scheduling, which is mainly affected by pore size and porosity; Consequently, it could be expressed as an equivalent depth of water and then converted to a volume for irrigation water requirements depending on the root-zone depth of cultivated plants and the field area. Moreover, soil water balance and irrigation intervals could be estimated by monitoring evapotranspiration and soil water depletion or surplus.

The curves presented in Fig. 1 indicate that the PE successfully simulated the SWCC of the specified soil for both ES and θ, in contrast to both FX and MVG, which include only ES. The regression equations of the simulated curves and the values of r, R^2, and LF are provided in Fig. 1 A. The results presented in Fig. 1 revealed that the PE produced a smooth curve with a very close fit to the measured data, and the predicted dependent variable (WC) was highly correlated and very sensitively affected by the independent factor (ψ). It is worth mentioning that the upper part of the curve in Fig. 1 is the most important part of the curve in agricultural sector because it controls soil water availability for plant uptake (FC and PWP). In this regard, Rabot et al. (2018) showed the details of the upper part of the pF curve. The main two limitations of the PE are a clay texture and the 1500 kPa range of ψ. Because of these potential limitations, we attempted to validate the PE over the full range of ψ and for different soil textures. Another limitation is that the PE was not tested for sandy soil, which represent the Egyptian deserts; therefore, further studies are needed. Consequently, Rastgou et al. (2020) stated that the method should be tested further with different datasets to evaluate its performance through soil and water investigations.

The next three steps were to validate the PE with the low range of ψ (i.e., to show air entry inflection point and FC) and with the entire range of ψ (from ψ at saturation up to close to air-dried soil) to show all the shape features of the curve for different soils, and to compare its fit with the most common models, i.e., MVG and FX. In this respect, Rahimi et al. (2015) reported that FX and VG are the most flexible equations to fit the measured data.

Models comparison

We compared the results of the PE with those of the most general and common SWCC models. Based on the previous discussion, we believe that it is well justified to focus the comparison on MVG, FX, and PE. In contrast to other models, those models make it possible to simulate the curve based on very limited data (only WC and ψ). Because of the lack of information on soil properties associated with model parameters, we decided to not investigate the physical meaning of the parameters and allowed them to change to achieve the best possible fit. Under certain assumptions, this can be correct if the equation does not initially depend of specified soil parameters, as in our case (MVG, FX, and PE).

Although MVG and FX are widely accepted, they suffer from some limitations due to the difficulties in calculating the saturation point associated with log 0 (i.e., ψ =0 at saturation). The general mathematical forms of MVG and FX are provided in Table 2.

Table 2. The mathematical expressions of the MVG and FX models.

Model	Equation	Free unknown parameters
MVG	$ES = \left[\frac{1}{1+(\alpha_2\psi)^{n_2}}\right]^{m_2}$	$\alpha_2; n_2; m_2$
FX	$ES = \frac{1}{\left[ln\left(e+\left(\frac{\psi}{\alpha_3}\right)^{n_3}\right)\right]^{m_3}}$	$\alpha_3; n_3; m_3$

The approach utilized overcomes such a limitation, and one more parameter was added to increase the ability of PE to precisely fit a range of soil data. The advantage of the PE is its utilization as it is with or without NWC or ES (WC can be used directly), which makes it easier to determine the soil moisture constants (FC and PWP)—this approach does not require the forcing of the matric ψ value to be zero at a value of 1 of ES (this is a condition of both FX and VG). The PE works with any value of ψ, even zero because it calculates the soil ψ value plus 1. The inclusion of the additional fitting parameter in the numerator (b) of the equation improved the simulation of the inflection points of the curve. In addition, the PE does not require previous determination of air-entry ψ or RWC, which are somewhat difficult to determine, and the values were not accurate, as mentioned previously. Perhaps this is the reason that the PE calculation can be done by any calculation method in the STATISTICA program, and for all data, unlike the case of MVG and FX, in some data, only the simplex method works with them.

Total four typical curves, these are all that was found in UNSODA database (Leij et al., 1996), were used to evaluate the performance of MVG, FX, and PE models in the low range of ψ. The figures, regression equations and obtained r, R^2, and LF values were presented in Appendix A (Figures A1-A4). The average values of r, R^2, and LF of the three studied models, were presented in Appendix B (Table B). The simulated curves and calculated statistical parameters clearly indicated that all three studied equations showed good fit to the measured data for all SWCCs.

It should be noted that FX model was established based on calculations of ES on the basis of mass, not volume, unlike the case of MVG and PE. Such point was not adopted because some used database did not include the value of bulk density, so the data was taken as it is and ES values were calculated. A comprehensive comparison of the fit of the desired models was evaluated based on three statistical tools, r, R^2, and LF. Selected data, to represent different soil textures for a typical measured SWCC, were used to test the model capabilities. For a reasonable comparison, the selection of the SWCC database was based on three conditions: a suitable number of points (enough to represent the curve), the full range of ψ, and a range of soil textures. The parameters of the MVG and FX models were allowed to change according to measured data for the purpose of obtaining the best simulation of the shape features of the SWCC and for unbiased comparison. The published measured data of the SWCC were obtained from Jackson et al. (1965), Jackson et al. (1965), Sillers and Fredlund (2001), Lu (2016), and Ghorbel and Leroureil (2006) for Figures. 2, 3, 4, 5, and 6, respectively. Figures 2–6 show the measured data and regression curves of the SWCC and the values of r, R^2, and LF for loam (two soils), sandy loam, silty, and clay soil textures, respectively.

Fig. 2 shows that MVG had the best fit for the two ends of the curve; PE showed the best fit in the middle and at the lower end of the curve (at high ψ). Generally, MVG showed the best fit, followed by PE and then FX for the different types of loam soil. Fig. 3 revealed that PE showed the best fit and produced a very smooth S-curve followed by FX and MVG for the other loam soil. According to Fig. 4, the PE and FX showed similar results and they had a better fit compared with MVG for the sandy loam soil. Furthermore, the PE simulated the curve in the section with a very rapid decrease for the relatively coarse-textured soil. Fig. 5 shows that PE demonstrated the best fit followed by MVG and FX. Based on Fig. 6, MVG showed the best fit followed by PE and FX for clay soil.

In this study, the model validation was limited only by its applicability regarding the ψ range and soil texture. The limitation of any provided equation is its fit across the entire range of ψ (from 0 to 10^6 kPa) based on satisfactory values of r, LF, and R^2 between estimated and measured values and the ability to be used for different soils. Fredlund and Xing (1994) and Jiang et al. (2020) reported that difficulties exist in the application of an available equation likely because the parameters of the equation are not individually related to the shape features of the SWCC; therefore, the lack of physical meaning for the fitting parameters is thus undesirable (Gitirana and Fredlund, 2004).

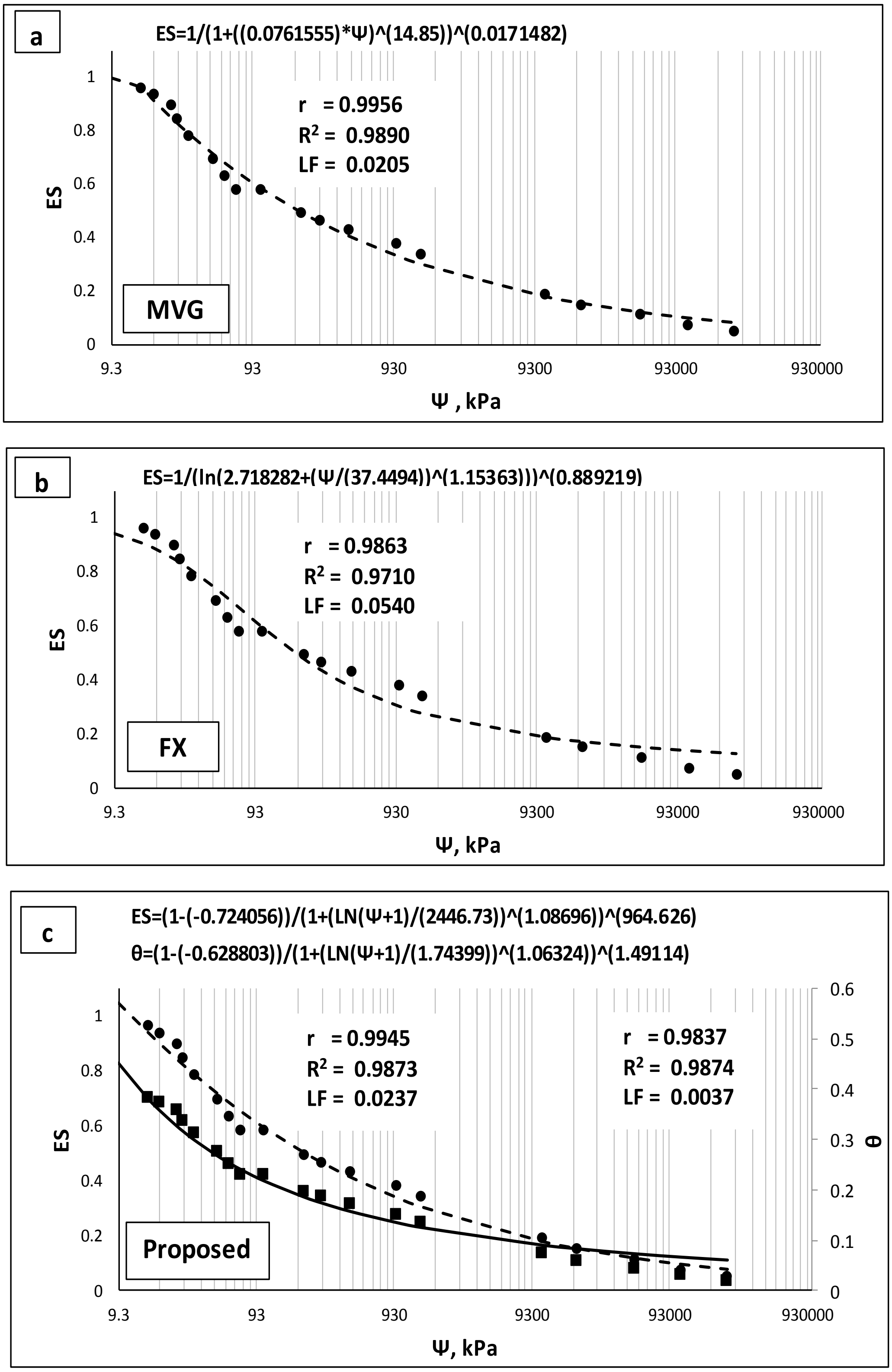

Fig. 2. Comparison of the fit of equations (MVG, FX, and PE, respectively) for loam soil 1 (Ghorbel and Leroureil, 2006).

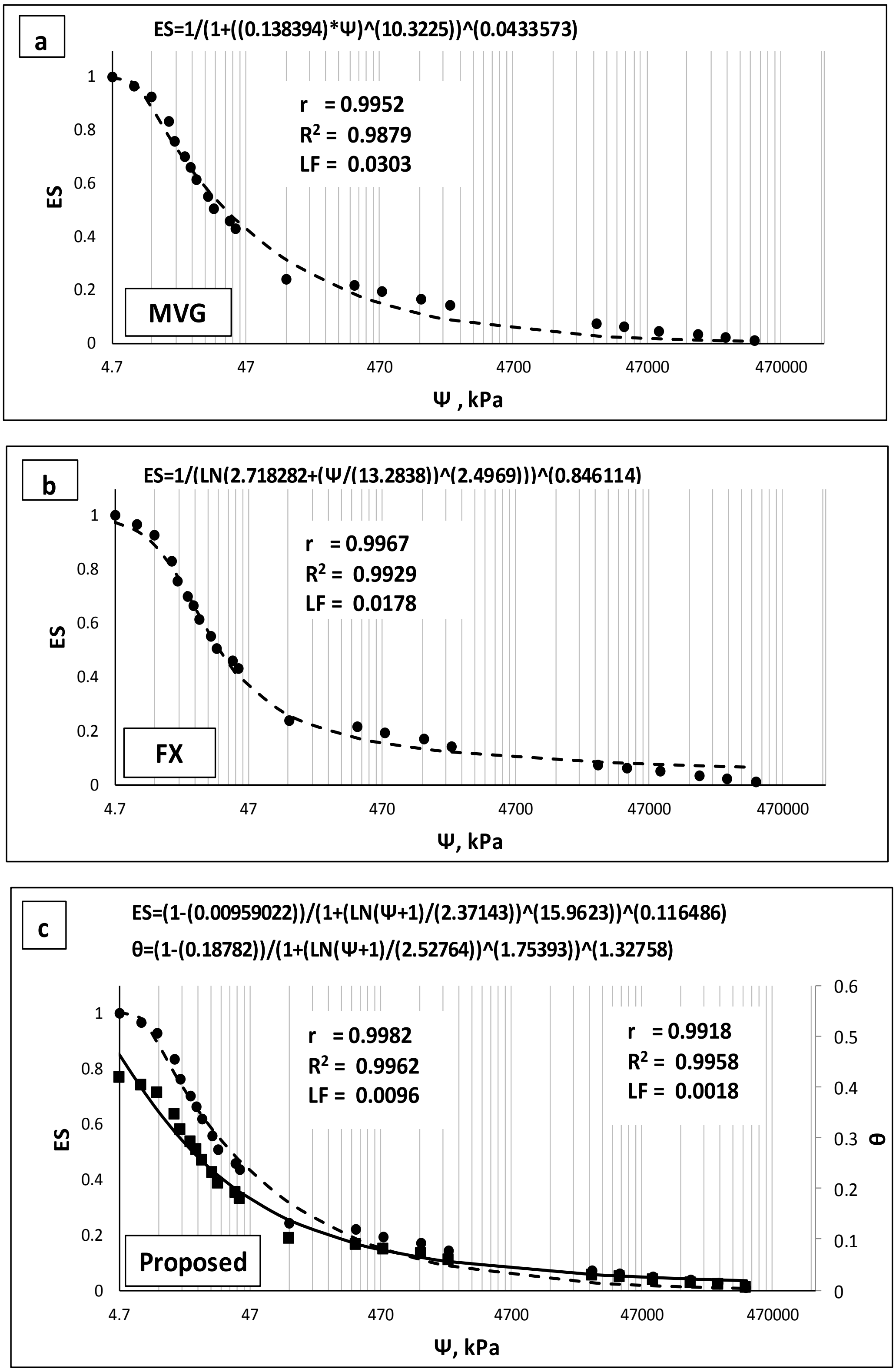

Fig. 3. Comparison of the fit of equations (MVG, FX, and PE, respectively) for loam soil 2 (Ghorbel and Leroureil, 2006).

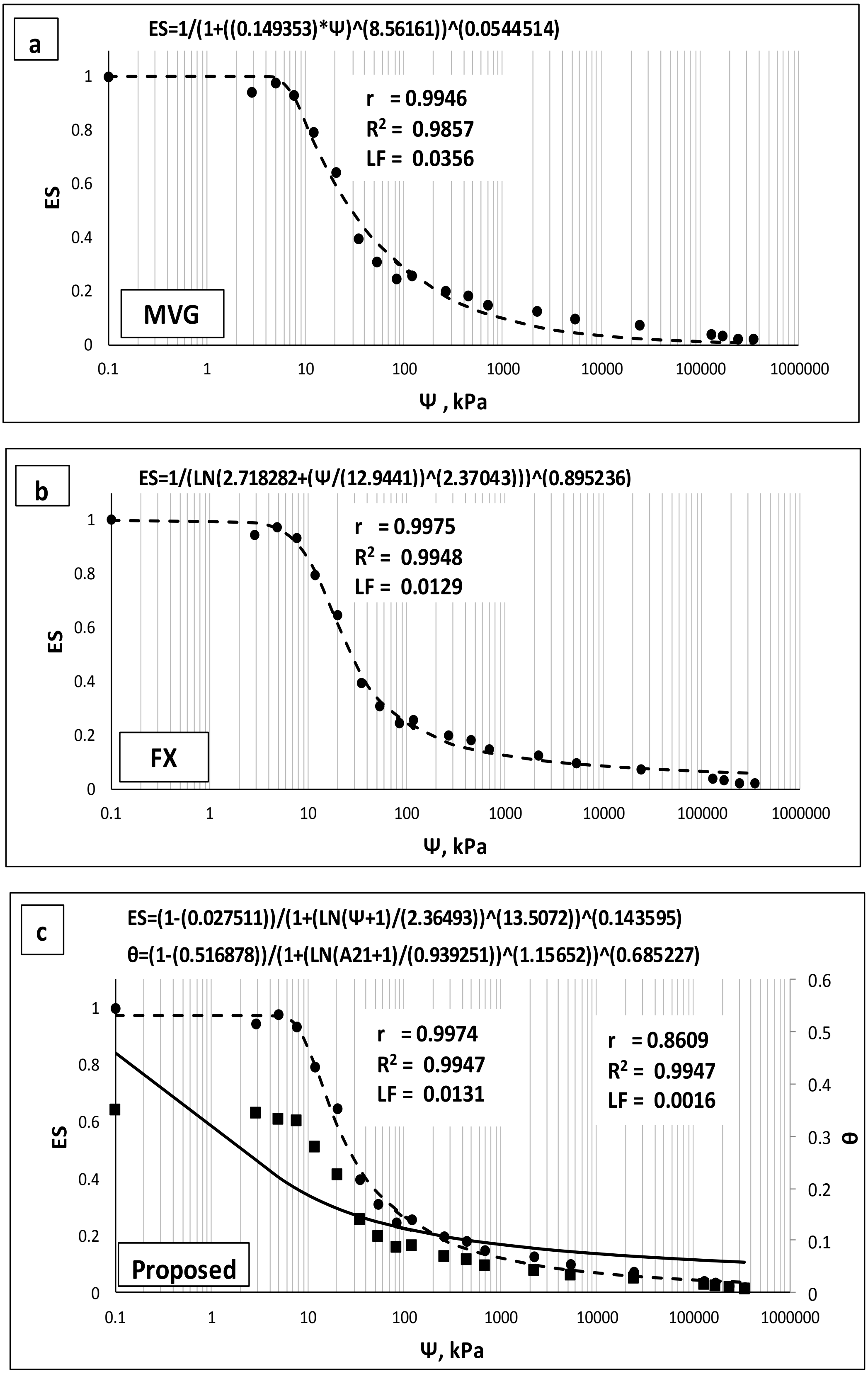

Fig. 4. Comparison of the fit of equations (MVG, FX, and PE, respectively) for sandy loam soil (Sillers and Fredlund, 2001).

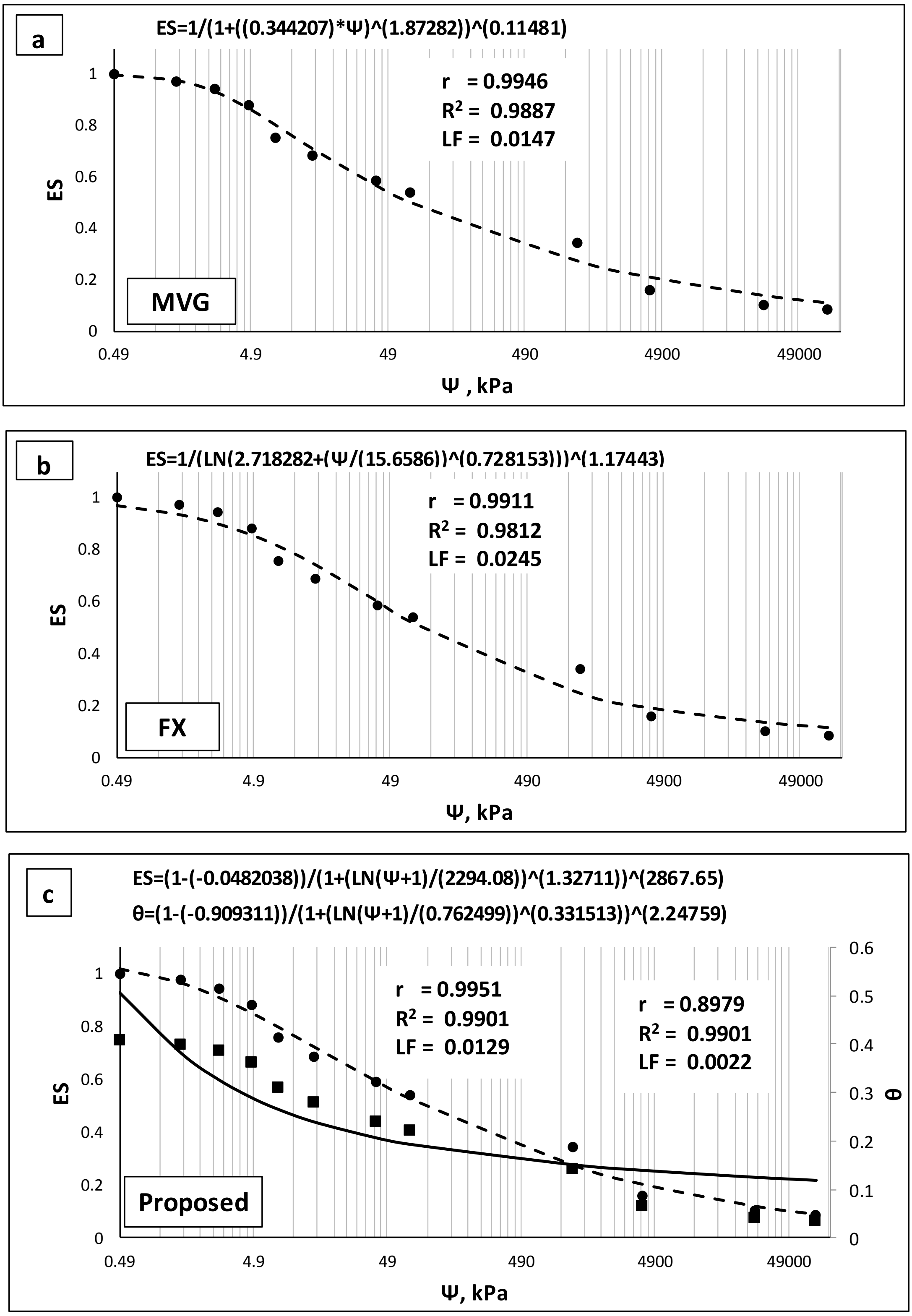

Fig. 5. Comparison of the fit of equations (MVG, FX, and PE, respectively) for clay soil (Fredlund and Xing, 1994.

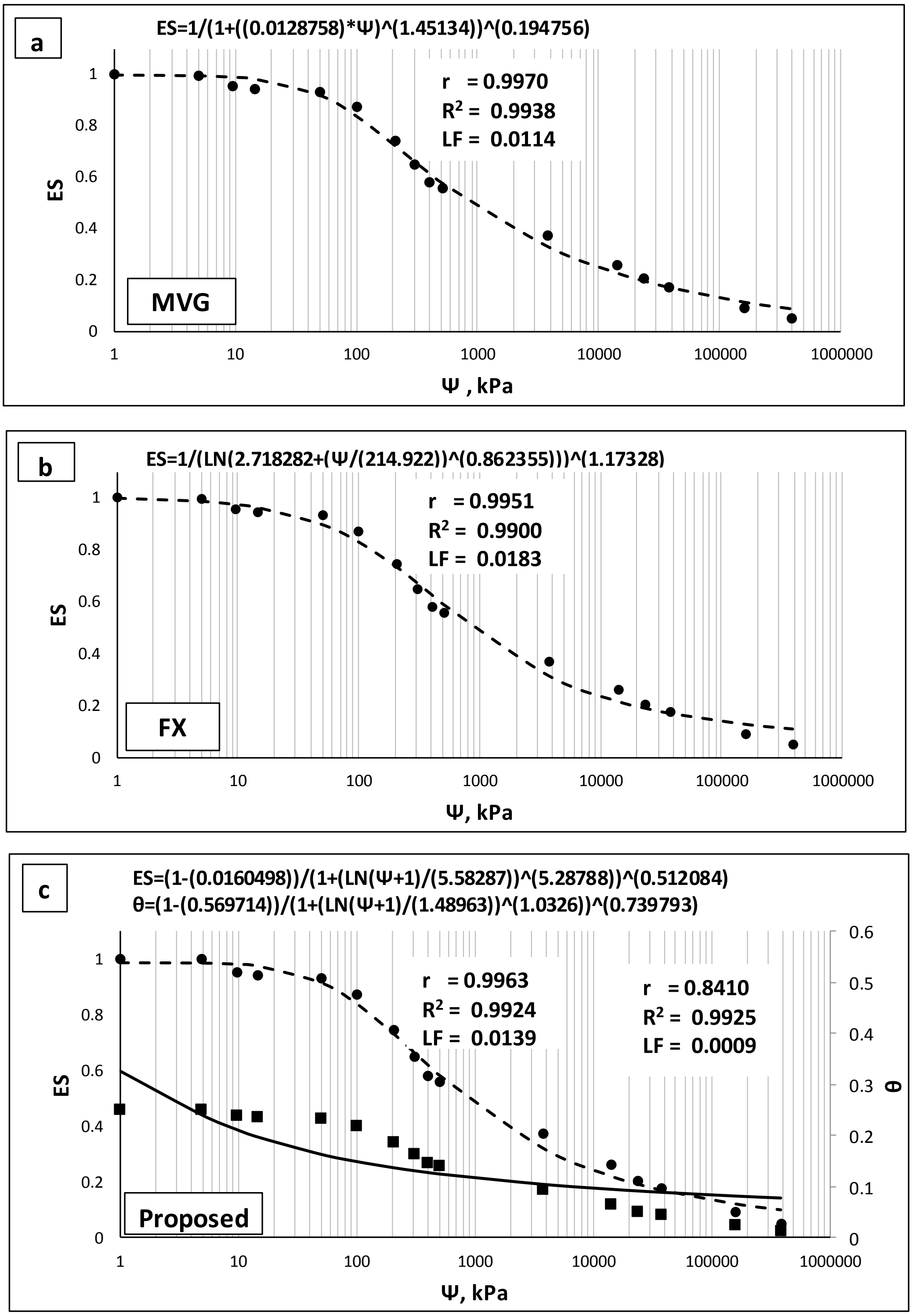

Fig. 6. Comparison of the fit of equations (MVG, FX, and PE, respectively) for clay soil (Lu, 2016).

We believe that the most important advantage of the PE was not to force the curve to cross between 1 ES and 0 ψ, as was done by MVG and FX (ψ = 0 will result in a value of 1 for both equations). Such a condition is correct theoretically, but practically this is not the case because if the saturation point is not measured accurately, it affects the whole curve. In other words, this condition makes the two equations strongly dependent on one point (if saturation occurs). The term ψ+1 overcomes the problems associated with log 0. In the case of saturation, the curves in Fig. 4 a and b started from zero in the MVG and FX simulation, but in Fig. 4 c, the PE curve is between the measured points, which increases the flexibility and reliability of the PE, especially in the upper complex part of the curve (horizontal line, inflection point and steep slope). Moreover, the performance of the PE in the middle section of the curve was very good, i.e., with a rapid decrease in relatively coarse-textured soil (Fig. 4), a moderate decrease in medium-textured soils (Fig. 2, 3, and 5), and a slow decrease in relatively fine-textured soil (Fig. 6).

The average values of r, R^2, and LF of MVG, FX, and PE are presented in Table 3, which clearly indicates that PE performed better than MVG and FX. It is worth mentioning that Leong and Rahardjo (1997) reported that most of the SWCC models provided a reasonable fit of the SWCC data but only in the low and intermediate ψ ranges.

Table 3. Average values of statistical tools (r, R^2, and FL), for the MVG, FX, and PE models of different soil textures (i.e., data presented in Figures 2-6).

Equation	MVG			FX			PE		
Statistical tool	r	R^2	LF	r	R^2	LF	r	R^2	LF
Average value	0.9954	0.9890	0.0225	0.9933	0.9860	0.0255	0.9963	0.9941	0.0146

As shown in Table 3, the PE showed the highest values of r and R^2 and the lowest value of LF, followed by MVG and FX. Superior results were generally achieved with PE compared with MVG and FX. Such results indicate that the MVG, FX and PE are valid when both inter-aggregate pores (micropores) and macropores exist between the soil aggregates are active (e.g., different soil textures), as explained by Simunek et al. (2003) in their discussion about dual-porosity and dual-permeability models of non-equilibrium and preferential flow.

4. Conclusions

The study introduced a modification of FX with four unknown parameters (i.e., PE) to gain more flexibility and applicability and to be suitable for soil science and agriculture applications rather than the civil engineering sector. For these reasons, the experimental SWCC was measured using volumetric WC. PE was developed based on laboratory measurements of clay soil to represent the types of soil around the Nile River in Egypt for a specific limited range of ψ (including saturation, FC, and the PWP). The PE was validated through a wide range of soil textures from very wet to very dry soil. The PE was compared with the most noteworthy SWCC models, i.e., MVG and FX, according to their capability and flexibility to fit various measured data over the full range of ψ. Different statistical tools and graphical presentations were employed to ensure the accuracy of the obtained regression equations. In conclusion, the PE is superior to the other models and should be used to generate SWCCs. Further studies are needed to evaluate the ability of the PE to simulate SWCCs for Egyptian sandy soils and to establish further essential relationships and applications, such as the soil water balance through the soil–water–plant–atmosphere continuum and the hydraulic conductivity of unsaturated soils.

5. Declaration of Funding:

This research did not recieve any speciefic funding.

6. Conflict of interest:

Thr author declare no conflict of interst.

7. Availability of data:

The data that support this study are available in the article and accompanying online supplementary material.

8. References

Abou hussien EA; Ismail M; Omran WM; Abou Alfotoh M (2020). Water harvesting for sustainable development of el-hraka basin in the north-western coast of Egypt. Egypt. J. Soil Sci. (60)3:263-276. DOI: 10.21608/ejss.2020.31570.1361

Achieng KO (2019). Modelling of soil moisture retention curve using machine learning techniques: Artificial and deep neural networks vs support vector regression models. Computers & Geosciences (133) 104320: 1-17. doi.org/10.1016/j.cageo.2019.104320

Assouline S, Tessier D, Bruand A (1998). A conceptual model of the soil water retention curve. Water Resour. Res. (34): 223-231. doi.org/10.1029/97WR03039

Bassouny MA, Abbas MH (2019). Role of biochar in managing the irrigation water requirements of maize plants: the pyramid model signifying the soil hydrophysical and environmental markers. Egypt. J. Soil Sci. (59)2: 99- 115. DOI: 10.21608/ejss.2019.9990.1252

Black GA, Evans DD, White JL, Ensminger LE, Clerk FE (1965). Methods of soil analysis. Parts, 1. American society of Agronomy Madison, USA.

Brooks RH, Corey AT (1964). Hydraulic properties of porous media. Hydrology Paper, No. 3, Colorado State University, Fort Collins, Colorado, USA.

Brutsaert W (1966). Probability laws for pore size distributions. Soil sciences (101): 85-92.

Burdine NT (1953). Relative permeability calculations for pore size distribution data. J. Petroleum Tech. 5: 71–78. doi.org/10.2118/225-G

Chai J, Khaimook P (2020). Prediction of soil-water characteristic curves using basic soil properties. Transportation Geotechnics (22) 100295: 1-11. doi.org/10.1016/j.trgeo.2019.100295

Campbell GS (1974). A simple method for determining unsaturated conductivity from moisture retention data. Soil Sci. 117 (6): 311-315. doi.org/10.1097/00010694-197406000-00001

Dane JH, Hopmans JW (2002). Water retention and storage. In Methods of soil analysis. Part 4. Physical methods (Dane J H, Topp G C). SSSA book series 5, Madison, WI. pp. 671–720.

Elbana M, Refaie KM, El-Shirbeny MA, Abdel Rahman MAE, Abdellatif B, El-Gendy R, Attia W (2019). Indirect estimation of deep percolation using soil water balance equation and nasa land simulation model (lIS) for more sustainable water management. Egypt. J. Soil. Sci. (59)4: 363- 383. DOI:10.21608/EJSS.2019.17427.1310

El-Nady MA (2015). Effect of different tillage practices and two cropping patterns on soil properties and crop productivity. Egypt. J. Soil Sci. (55)4: 425- 440. DOI:10.21608/EJSS.2015.1560

Eyo EU, Ngambi S, Abbey SJ (2020). An overview of soil-water characteristic curves of stabilized soils and their influential factors. J. King Saud Univ. Eng. Sci. doi.org/10.1016/j.jksues.2020.07.013

Farrel D, Larson WE (1972). Modelling the pore structure of porous media. Water Resour. Res. 8 (3): 699-706. doi.org/10.1029/WR008i003p00699

Fredlund DG, Xing A (1994). Equations for the soil-water characteristics curve. Canadian Geotech. J. 31: 521-532. doi.org/10.1139/t94-061

Fredlund DG, Xing A, Huang S (1994). Predicting the permeability function for unsaturated soils using the soil–water characteristic curve. Canadian Geotech. J. 31: 533-546. https://doi.org/10.1139/t94-062

Fredlund DG, Sheng D, Zahao J (2011). Estimation of soil suction from the soil-water characteristic curve. Canadian Geotech. J. 48: 186-198. doi.org/10.1139/T10-060

Gardner WR (1958). Some steady state solutions of the unsaturated moisture with application to evaporation from a water table. Soil Sci. 85: 228-232. doi.org/10.1097/00010694-195804000-00006

Gavin HP (2019). The Levenberg-Marquardt algorithm for nonlinear least squares curve-fitting problems. Duke Univ. 1-19. http://people.duke.edu/~hpgavin/ce281/lm.pdf

Ghorbel S, Leroureil S (2006). An elasto-plastic model for the unsaturated soils. Unsaturated soil. Geotechn. ASCE Special Pub. 2(147): 1908-1919. doi.org/10.1061/40802(189)161

Gitirana G, Fredlund DG (2004). Soil-water characteristic curve equation with independent properties. J. Geotech. Geoenviron. Eng., ASCE. 130(2): 209-212. doi.org/10.1061/(asce)1090-0241(2004)130:2(209)

Kosugi K (1994). Three- parameter lognormal distribution model for soil water retention. Water Resour. Res. 30 (4): 891-901. doi.org/10.1029/93WR02931

Jackson RD, Reginato RJ, Van Bavel CHM (1965). Comparison of measured and calculated hydraulic conductivities of unsaturated soils. Water Resour. Res. 1(3): 375-380.

Jiang X, Wu L, Wei Y (2020). Influence of fine content on the soil–water characteristic curve of unsaturated soils. Geotech. Geologic. Eng. 38:1371–1378. doi.org/10.1007/s10706-019-01096-5

Leij FJ, Alves WJ, van Genuchten MTh, William JR (1996). Unsaturated Soil Hydraulic Database, UNSODA 1.0 User's Manual. Report EPA/600/R-96/095, U.S. Environmental Protection Agency. Ada, Oklahoma. Pages 77 and 93.

Leong EC, Rahardjo H (1997). Review of soil-water characteristic curve functions. J. Geotech. Geoenviron. Eng., ASCE. 123(12): 1106-1117. https://doi.org/10.1061/(ASCE)1090-0241(1997)123:12(1106)

Lourakis MIA (2005). A brief description of the Levenberg-Marquardt algorithm implemented by levmar. https://users.ics.forth.gr/~lourakis/levmar/levmar.pdf

Lu N (2016). Generalized soil water retention equation for adsorption and capillarity. J. Geotechn. Geoenviron. Eng., ASCE. 142(10): 1-15. doi.org/10.1061/(ASCE)GT.1943-5606.0001524

Maulem Y (1976). A new model for predicting the hydraulic conductivity of unsaturated porous medial. Water Resour. Res. (12): 513-522.

Pansu M, Gautheyrou J (2006). Handbook of soil analysis mineralogical, organic and inorganic methods. Springer, New York. Chapter 2: 15-63.

Rabot E, Wiesmeier M, Schluter S, Vogel HJ (2018). Soil structure as an indicator of soil functions: A review. Geoderma (314): 122–137. doi.org/10.1016/j.geoderma.2017.11.009

Rahimi A, Rahardjo H, Leong E (2015). Effects of soil-water characteristic curve and relative permeability equations on estimation of unsaturated permeability function. Soils and Foundations 55(6):1400–1411. Japan. Geotech. Soc. http://dx.doi.org/10.1016/j.sandf.2015.10.006

Rastgou M, Bayat H, Mansoorizadeh M, Gregory AS (2020). Estimating the soil water retention curve: Comparison of multiple nonlinear regression approach and random forest data mining technique. Computers and Electronics in Agriculture (174) 105502: 1-13. doi.org/10.1016/j.compag.2020.105502

Rousseva S, Kercheva M, Shishkov T, Lair GJ, Nikolaidis NP, Moraetis D, Krám P, Bernasconi SM, Blum WEH, Menon M, Banwart SA (2017). Soil water characteristics of European soilTrEC critical zone observatories. Advances in Agronomy (142): 29-72. URL 10.1016/bs.agron.2016.10.004

Saxton KE, Rawls WJ, Romberger JS, Papendick RI (1986). Estimating generalized soil-water characteristics from texture. Soil Sci. Soc. America J. 50: 1031-1036. https://hrsl.ba.ars.usda.gov/SPAW/Help/Article.htm

Sheta M. H. and Fayed M. H. (2021). Productivity and water use efficiency of summer squash crop under two methods of irrigation water application. Egypt. J. Soil Sci. 61(1):1-11. DOI: 10.21608/ejss.2020.48343.1404

Sillers WS, Fredlund DG (2001). Statistical assessment of soil-water characteristic models. Canadian Geotech. J. 38 (6): 1297-1313. doi.org/10.1139/t01-066

Simunek J, Jarvis N J, Van Genuchten M Th, Gardenas A (2003). Review and comparison of models for describing non-equilibrium and preferential flow and transport in the vadose zone. J. Hydrology 272 (1-4): 14–35. doi.org/10.1016/S0022-1694(02)00252-4

Smith KA, Mullins CE (2001). Soil and environmental analysis: Physical methods. 2nd ed. Chapter 3 (Water release characteristic). doi.org/10.1201/9780203908600

Tinjum JM, Benson HC, Blotz LR (1997). Soil-water characteristic curves for compacted clays. J. Geotech. Geoenviron. Eng., ASCE. 123(11): 1060-1069. doi.org/10.1061/(ASCE)1090-0241(1997)123:11(1060)

van Genuchten MT (1980). A closed-form equation for predicting the hydraulic conductivity of unsaturated soils. Soil Sci. Soc. America J. 44: 892-898. doi.org/10.2136/sssaj1980.03615995004400050002x

van Genuchten MT, Leij F, Yates S (1991). The Retc code quantifying the hydraulic functions of unsaturated soils. Rep. EPA⁄600⁄291⁄065, U.S. EPA, Ofc. of Res. and Devel., Washington, D.C.

Visser WC (1968). An empirical expression for the desorption curve. In Water in the Unsaturated Zone: Proceeding of Wageningen Symposium, PE Rijtema and H Wassink, Eds., vol. 1, pp. 329–335, IASH/AIHS, Unesco, Paris, France.

Williams J, Prebble RE, Williams WT, Hignett CT (1983). The influence of texture, structure and clay mineralogy on the soil moisture characteristic. Australian J. Soil Res. 21: 15-32. doi.org/10.1071/sr9830015

Appendix A

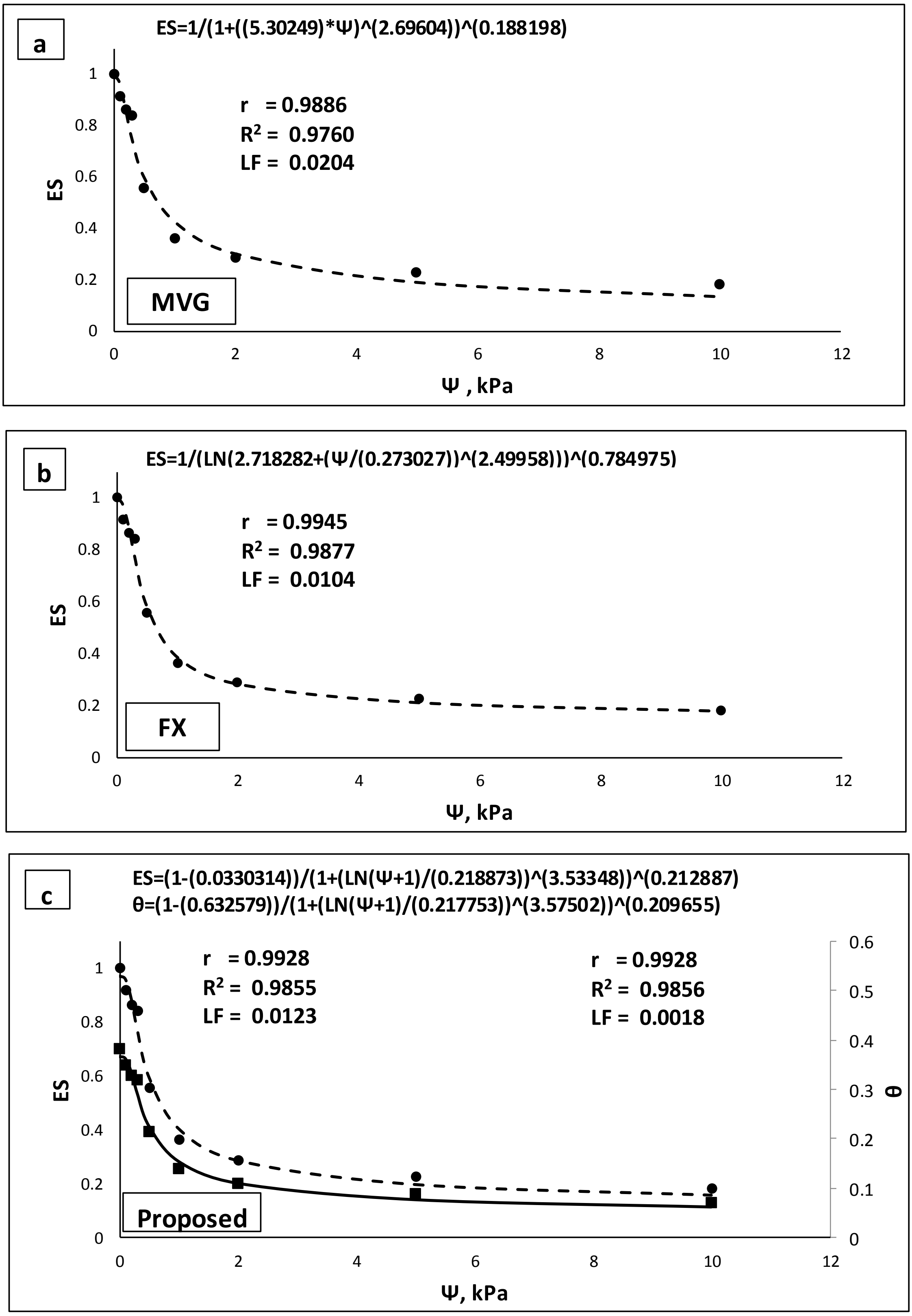

Fig. A1. Measured and simulated SWCC using MVG, FX and PE for soil 1 (Leij et al., 1996).

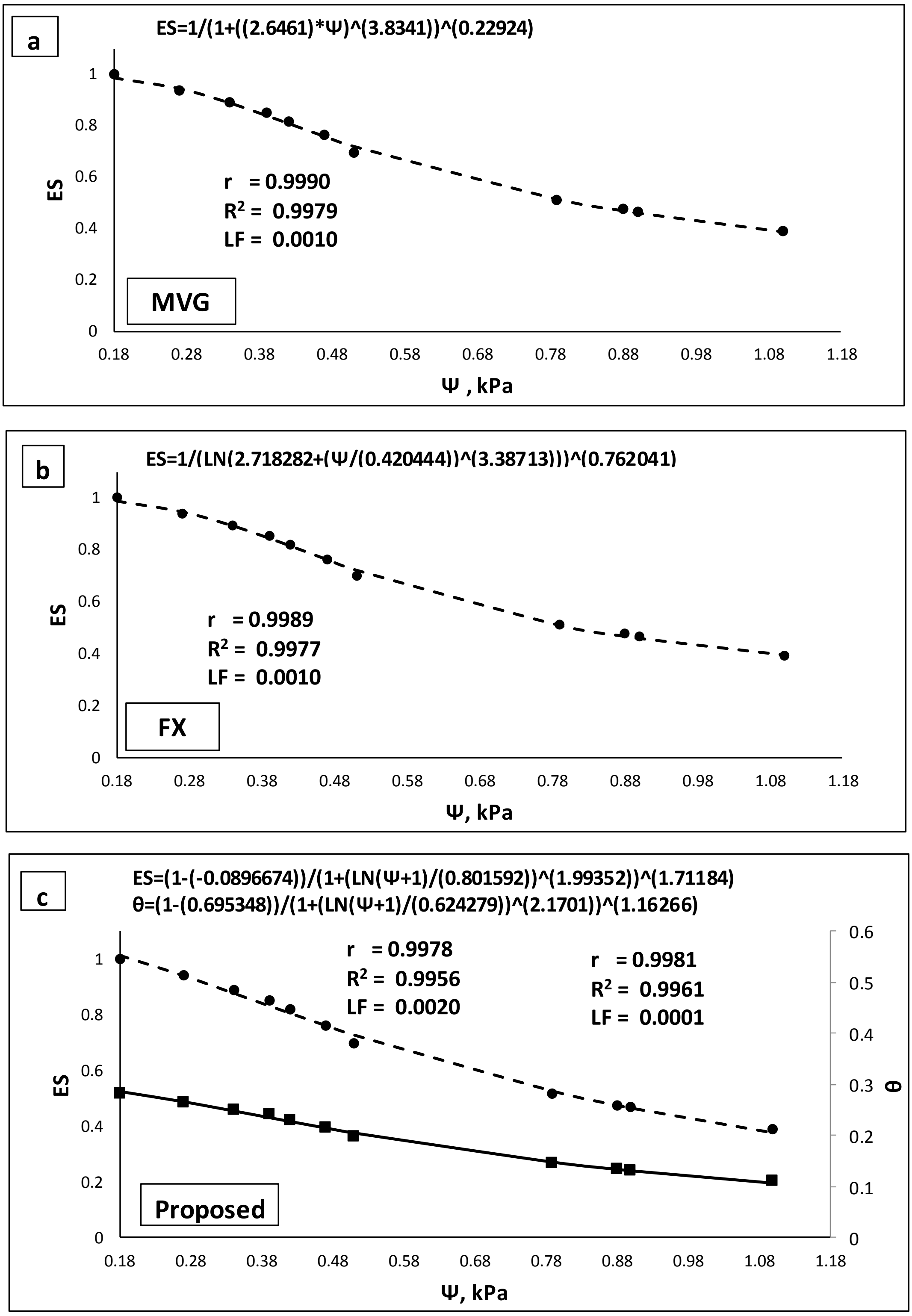

Fig. A2. Measured and simulated SWCC using MVG, FX and PE for soil 2 (Leij et al., 1996).

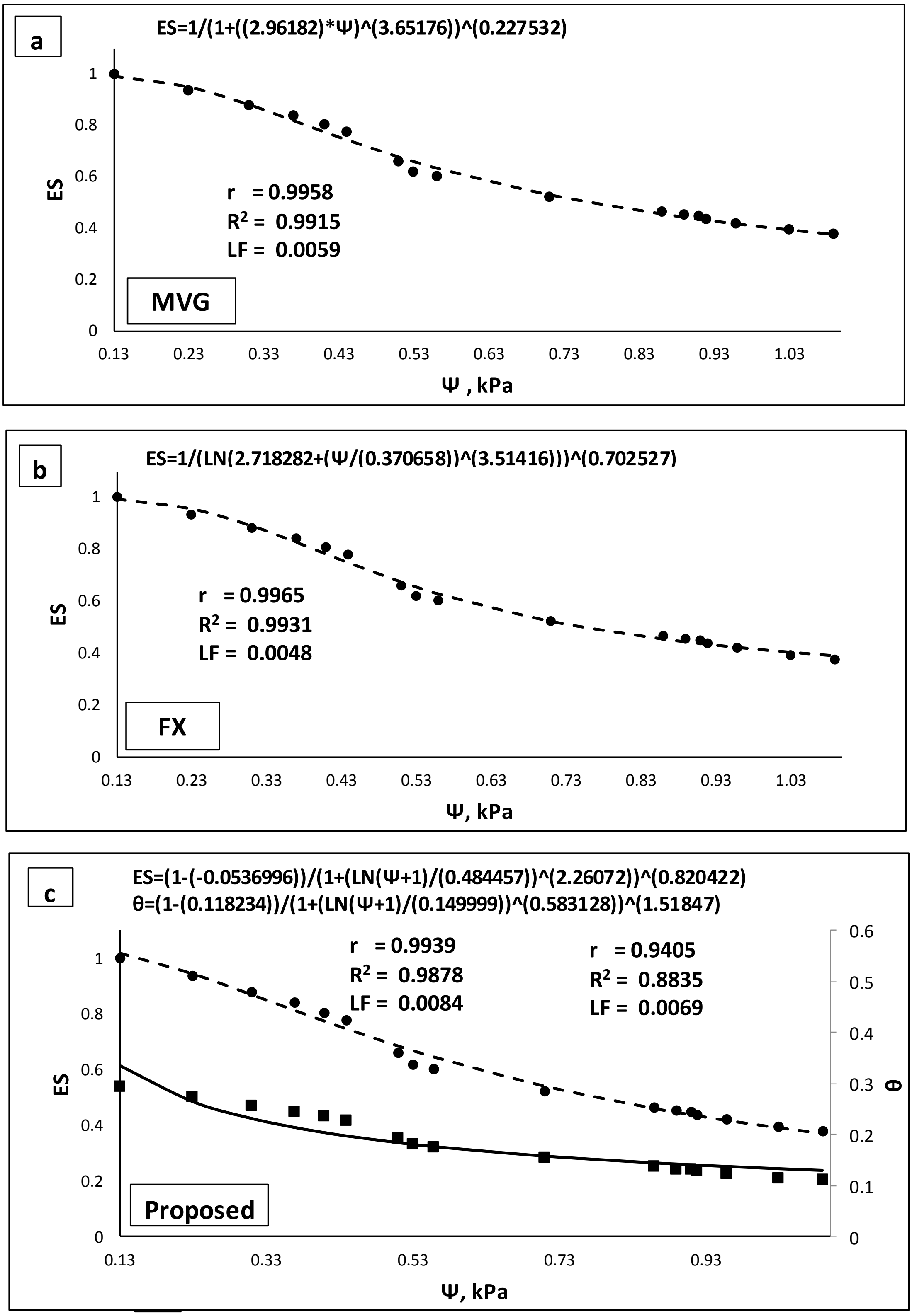

Fig. A3. Measured and simulated SWCC using MVG, FX and PE for soil 3 (Leij et al., 1996).

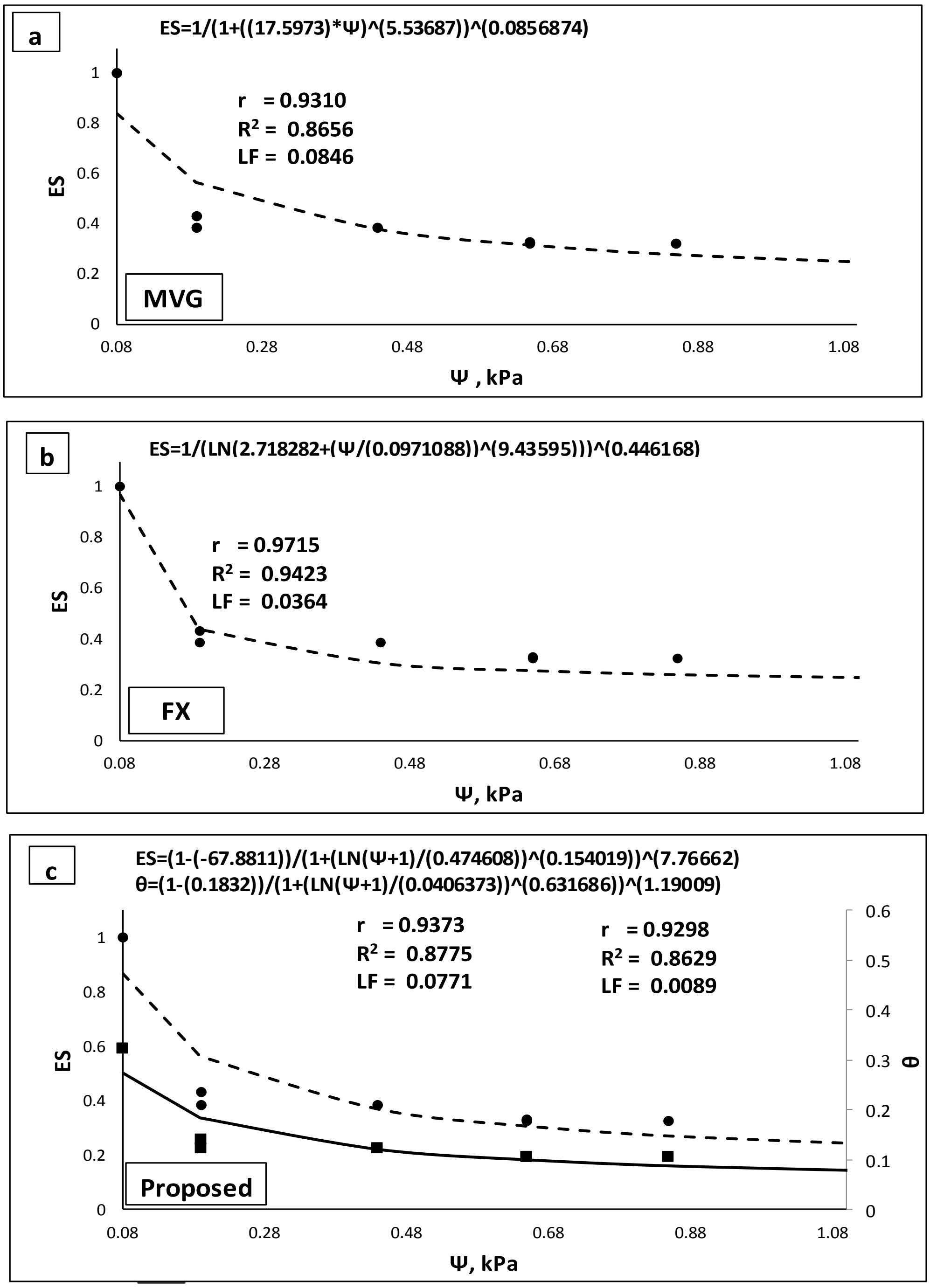

Fig. A4. Measured and simulated SWCC using MVG, FX and PE for soil 4 (Leij et al., 1996).

Appendix B

Table B. Average values of statistical tools (r, R^2, and FL), for the MVG, FX, and PE models of different soils (i.e., data presented in Figures A1-A4).

Equation	MVG			FX			PE		
Statistical tool	r	R^2	LF	r	R^2	LF	r	R^2	LF
Average value	0.9786	0.9578	0.0280	0.9904	0.9802	0.0132	0.9805	0.9616	0.0250